

# Cross-Correlation between UHECR Arrival Distribution and Large-Scale Structure

Hajime Takami<sup>1,2</sup>, Takahiro Nishimichi<sup>1</sup>, Kazuhiro Yahata<sup>1</sup>,  
and Katsuhiko Sato<sup>2,3</sup>

<sup>1</sup> Department of Physics, School of Science, the University of Tokyo, 7-3-1 Hongo, Bunkyo-ku, Tokyo 113-0033, Japan

<sup>2</sup> Institute for the Physics and Mathematics of the Universe, the University of Tokyo, 5-1-5, Kashiwanoha, Kashiwa, Chiba 277-8582, Japan

<sup>3</sup> Department of Physics, School of Science and Engineering, Meisei University, 2-1-1 Hodokubo, Hino-shi, Tokyo 191-8506, Japan

E-mail: takami@utap.phys.s.u-tokyo.ac.jp

**Abstract.** We investigate correlation between the arrival directions of ultra-high-energy cosmic rays (UHECRs) and the large-scale structure (LSS) of the Universe by using statistical quantities which can find the angular scale of the correlation. The Infrared Astronomical Satellite Point Source Redshift Survey (IRAS PSCz) catalog of galaxies is adopted for LSS. We find a positive correlation of the highest energy events detected by the Pierre Auger Observatory (PAO) with the IRAS galaxies inside  $z = 0.018$  within the angular scale of  $\sim 15^\circ$ . This positive correlation observed in the southern sky implies that a significant fraction of the highest energy events comes from nearby extragalactic objects. We also analyze the data of the Akeno Giant Air Shower Array (AGASA) which observed the northern hemisphere, but the obvious signals of positive correlation with the galaxy distribution are not found. Since the exposure of the AGASA is smaller than the PAO, the cross-correlation in the northern sky should be tested using a larger number of events detected in the future. We also discuss the correlation using the all-sky combined data sets of both the PAO and AGASA, and find a significant correlation within  $\sim 8^\circ$ . These angular scales can constrain several models of intergalactic magnetic field. These cross-correlation signals can be well reproduced by a source model in which the distribution of UHECR sources is related to the IRAS galaxies.

PACS numbers: 95.85.Ry,98.70.Sa

## 1. Introduction

The origin of ultra-high-energy cosmic rays (UHECRs) above  $10^{19}$  eV has been an open problem in astroparticle physics. The highly isotropic distribution of their arrival directions and the deflection angles of UHECRs estimated in the Galaxy have indicated the extragalactic origin of them. In 1999, Akeno Giant Air Shower Array (AGASA) found a small-scale anisotropy of the arrival distribution of UHECRs above  $4 \times 10^{19}$  eV within  $2.5^\circ$ , which is comparable with its angular resolution [1]. The small-scale anisotropy can be interpreted as a signal of point-like sources.

Motivated by the AGASA result, many researchers have tested correlation between the arrival directions of UHECRs and the positions of several classes of astrophysical objects. The correlation with BL Lac objects was discussed by using the AGASA and Yakutsk data [2, 3, 4]. The authors of Refs. [5, 6] studied the correlation with infrared galaxies using *Infrared Astronomical Satellite Point Source Redshift Survey* (IRAS PSCz) catalog [7], and discussed the possibility that the AGASA events below  $\sim 10^{20}$ eV come from luminous infrared galaxies. In Ref. [8], the correlation with nearby active galactic nuclei (AGNs) listed in the *Rossi X-ray Timing Explorer* (RXTE) catalog of AGNs was investigated and no significant correlation was found. The authors of Ref. [9] made a comprehensive study of correlation with various classes of powerful extragalactic sources and found that BL Lac objects and unidentified gamma-ray sources might be correlated with the AGASA and Yakutsk data. The spatial correlation with the supergalactic plane has also been discussed and positive signals have been obtained [10, 11, 12]. On the other hand, High Resolution Fly's Eye (HiRes) reported no significant signal for any point-like sources [13, 14] and the correlation with BL Lac objects studied by Refs. [2, 3, 4] was not supported by the HiRes data [15]. Theoretically, several authors predicted the anisotropy of UHECR arrival distribution in future observations when UHECR source distribution follows the large-scale structure (LSS) of the Universe [16, 17, 18, 19]. Cosmic rays above  $8 \times 10^{19}$  eV lose their energies rapidly by interactions with cosmic microwave background (CMB) and therefore they cannot reach the earth from distant sources, typically above 100 Mpc (Greisen-Zatsepin-Kuz'min (GZK) mechanism [20, 21]). In other words, the GZK mechanism predicts positional correlation between such highest energy cosmic rays and nearby UHECR sources if the Universe is not magnetized. We predicted such positional correlation within a few degree scale even taking into account a structured intergalactic magnetic field (IGMF), which reproduces the observed structure of local Universe, and 5 yrs observation of the Pierre Auger Observatory (PAO) will unveil the local UHECR source distribution [18].

Recently, the PAO has reported correlation between the arrival directions of its 27 events above  $5.7 \times 10^{19}$ eV and the positions of nearby active galactic nuclei (AGNs) with  $3\sigma$  confidence level [22, 23]. This report showed that the isotropic distribution of the arrival directions of the highest energy cosmic rays is disfavored. This was also a clear evidence which indicated directly that UHECR sources are extragalactic objects

and can be regarded as the start of UHECR astronomy.

However, the interpretation of the PAO results is problematic. All of the PAO-correlated AGNs except Centaurus A are classified into Seyfert galaxies and Low-Ionization Nuclear Emission Regions (LINERs), which have much weaker activities than radio-loud AGNs, one of plausible candidates of UHECR sources [25]. Thus, it is an open question whether the PAO-correlated AGNs are really UHECR sources.

The PAO adopted the 12th edition of Veron-Cetty & Veron Catalog (VC catalog) of AGNs [24] for a correlation analysis. This catalog is a compilation of many astronomical catalogs of AGNs available in literature and therefore AGNs in the VC catalog are selected based on different criteria. In order to investigate the nature of UHECR sources, the authors of Ref. [29] analyzed the spatial correlation of the PAO events with hard X-ray selected AGNs compiled by the Swift satellite, an AGN catalog compiled based on a criterion. They found a significant correlation by using the 2 dimensional generalization of the Kolmogorov-Smilnov test (2D KS test).

More generally, the arrival directions of UHECRs are expected to correlate with a galaxy distribution, which is a representative of LSS of the Universe, if UHECR sources are some astrophysical objects. When a correlation with LSS is investigated, a catalog as homogeneous as possible is required. Ref. [19] studied correlation between the PAO events and LSS using the IRAS PSCz catalog. They showed that the PAO data is inconsistent with random distribution of UHECR sources at 98% confidence level and favors a modeled source distribution following LSS. They analyzed the similarity between the observed arrival distribution of UHECRs and mock one from their cosmic ray intensity map constructed based on the IRAS catalog using  $6^\circ \times 6^\circ$  angular bins. The bin size was determined by considering possible deflections of UHECRs by the IGMF in order to avoid the effect of the IGMF. Ref. [30] discussed the correlation with HI-selected galaxies by using 2D KS test and a significant correlation was found. The authors interpreted the result as an evidence that spiral galaxies are the hosts of UHECR sources and could suggest that newly born magnetars are the best candidates of UHECR sources. Note that 2D KS test cannot estimate the angular scale of a spatial correlation. These works are important steps toward the understanding of UHECR sources. However, if the angular scale is naturally found by another analysis without fixing the scale, we can obtain a better evidence of the correlation and information on intervening magnetic fields and the composition of UHECRs.

In this study, we investigate spatial correlation between the arrival directions of the observed highest energy cosmic rays and a galaxy distribution as a representative of LSS by using statistical quantities which need not to set an artificial angular scale and can estimate the angular scale of the correlation. We adopt the PAO data for cosmic rays observed in the southern hemisphere and the AGASA data for cosmic rays detected in the northern hemisphere. The HiRes is a UHECR observatory with the largest exposure in the northern hemisphere and recently, the HiRes reported no significant correlation with AGNs listed in the VC catalog in their data by using the same method as the PAO [28]. However, HiRes has not published the detailed data and, moreover, the analytical

estimation of the apertures of fluorescence detectors is more complicated than that of ground-based detectors. Thus, we do not consider the HiRes in this paper. We also check whether a source model associated with LSS can reproduce the cross-correlation signal and try to constrain the IGMF strength taking into account UHECR propagation in magnetized intergalactic space. This approach allows us to analyze the correlation taking account of the radial information of the positions of UHECR sources.

This paper is laid out as follows. In Section 2, we explain a galaxy catalog which represents LSS and UHECR samples used in this study, and our methods of the statistical analysis. In Section 3, we calculate cross-correlation function introduced in Section 2 between the arrival directions of the observed highest energy cosmic rays and the positions of nearby galaxy distribution, and discuss correlation with its angular scale. In Section 4, we construct a simple model of UHECR sources, check the reproducibility of the observed cross-correlation and try to constrain the IGMF strength. Finally, in Section 5, we discuss our results and make conclusions.

## 2. Sample data and Statistical Methods

### 2.1. Galaxy and UHECR Catalogs

We adopt the IRAS PSCz catalog of galaxies [7]. In order to represent the LSS of the Universe by galaxies, a uniform catalog of galaxies is appropriate. The IRAS catalog is a flux-limited catalog to contain 14,677 galaxies with redshift and covers a large fraction of the entire sky ( $\sim 84\%$ ). Almost all of the uncovered area is around the Galactic plane. Thus, this is a good catalog to study correlation between the arrival distribution of UHECRs and LSS.

As the observed data of the arrival directions of UHECRs, we adopt published data by the southern site of the PAO [23], which contains 27 events above  $5.7 \times 10^{19}$  eV, and data published by the AGASA with 57 events above  $4 \times 10^{19}$  eV [31]. The total exposure of the PAO is  $9.0 \times 10^3$  km<sup>2</sup> sr, and that of AGASA, which is the largest ground array in the northern hemisphere, is  $1.3 \times 10^3$  km<sup>2</sup> sr.

The apertures of cosmic ray experiments are not uniform, but the apertures of ground arrays only depend on the declination of the arrival directions of cosmic rays,  $\delta$ . Their exposures,  $\omega(\delta)$ , can be estimated analytically as [32]

$$\omega(\delta) \propto \cos(a_0) \cos(\delta) \sin(\alpha_m) + \alpha_m \sin(a_0) \sin(\delta), \quad (1)$$

where  $\alpha_m$  is given by

$$\alpha_m = \begin{cases} 0 & \text{if } \xi > 1 \\ \pi & \text{if } \xi < -1 \\ \cos^{-1}(\xi) & \text{otherwise} \end{cases} \quad (2)$$

and

$$\xi \equiv \frac{\cos(\theta) - \sin(a_0) \sin(\delta)}{\cos(a_0) \cos(\delta)}. \quad (3)$$

Here  $a_0$ , and  $\theta$  are the terrestrial latitude of a ground array and the zenith angle for an experimental cut. These values are  $a_0 = -35.2^\circ$ ,  $\theta = 60^\circ$  for the PAO [22, 23], and  $a_0 = 35^\circ.47'$ ,  $\theta = 45^\circ$  for the AGASA [1]. Fig. 1 represents the declination dependence of the exposures of both experiments and the combined experiment. The total exposure of the AGASA is about 7 times smaller than that of the PAO. These dependence of the exposures is taken into account throughout this paper.

## 2.2. Estimators of Statistical Quantities

A traditional statistical quantity in cosmology to investigate similarity between two distribution is cross-correlation function [33]. This function can be calculated from pair-counts between two distribution if the positions of all objects are known on the whole sky. Now we would like to calculate the cross-correlation function between the arrival directions of UHECRs and the positions of the IRAS galaxies. As explained above, the IRAS PSCz catalog has 16% of unobserved area (*mask*) and the apertures of the UHECR observatories depend on the declination of the arriving events, so that both apertures are not uniform. In such case, estimators of the cross-correlation function, which can infer the cross-correlation function in the case of uniform apertures have been adopted in observational cosmology.

We adopt

$$w_{\text{eg}}(\theta) = \frac{EG(\theta) - EG'(\theta) - E'G(\theta) + E'G'(\theta)}{E'G'(\theta)}, \quad (4)$$

as the estimator of the cross-correlation function, which is a modified version of that used in Ref. [35] originally suggested for auto-correlation function by Ref. [34].  $EG(\theta)$  is normalized pair-counts between galaxies in the IRAS catalog and cosmic ray events with the separation angle of  $\theta$ , which is obtained by dividing calculated pair-counts by  $N_e N_g$ , where  $N_e$  and  $N_g$  are the number of events and the number of galaxies, respectively.  $EG'(\theta)$ ,  $E'G(\theta)$ , and  $E'G'(\theta)$  are the similar pair counts, but  $G'$  and  $E'$  represent galaxies randomly put inside the observed sky and cosmic ray events randomly put with number density proportional to the detector apertures, respectively. These randomly put galaxies and events enable us to correct the effect of non-uniform apertures. These galaxies and events must be put with sufficiently large number to reflect the apertures. We consider 400,000 random distributed galaxies, and 200,000 and 400,000 randomly put events for the calculation of  $w_{\text{eg}}(\theta)$  using the PAO or AGASA data separately and the combined all-sky data, respectively. The width of the angular bin is set to be  $1^\circ$ , which is comparable with the angular resolution of the PAO [22, 23]. If there is no correlation,  $w_{\text{eg}}(\theta)$  is equal to zero. Positive value of  $w_{\text{eg}}(\theta)$  corresponds to positive correlation and vice versa. Thus, we search angular scales in which  $w_{\text{eg}}(\theta)$  is positive.

We also discuss the auto-correlation of galaxy distribution. We adopt an estimator of the auto-correlation function suggested by Ref. [34],

$$w_{\text{gg}}(\theta) = \frac{GG(\theta) - 2GG'(\theta) + G'G'(\theta)}{G'G'(\theta)}, \quad (5)$$

where  $GG(\theta)$ ,  $GG'(\theta)$ , and  $G'G'(\theta)$  are normalized pair-counts obtained by dividing calculated pair-counts by  $N_g(N_g - 1)/2$ ,  $N_gN'_g$ , and  $N'_g(N'_g - 1)/2$ , respectively.

### 3. Correlation with Nearby Galaxies

In this section, we search cross-correlation signals between the PAO and AGASA data, and the positions of the IRAS galaxies. The cross-correlation functions of the data defined in Section 2.2 are calculated and are compared with that calculated from event distribution randomly placed following the apertures of the detectors. We adopt the IRAS galaxies within  $z = 0.018$  as nearby galaxy distribution, which is the same criterion as analyses by the PAO [22, 23].

Fig.2 shows the galaxy distributions of the IRAS catalog within (*left*) and outside (*right*)  $z = 0.018$  with the arrival directions of the highest energy events observed by the PAO ( $E \geq 5.7 \times 10^{19}$  eV; *blue*) and AGASA ( $E \geq 4.0 \times 10^{19}$  eV; *green*,  $E \geq 9.5 \times 10^{19}$  eV; *red*) in equatorial coordinates. The classification of the AGASA data is for convenience when we discuss the combined data of the PAO and AGASA. The numbers of galaxies within and outside  $z = 0.018$  are 4419 and 10258, respectively. In the left figure, several nearby clusters of galaxies can be found. In the PAO data, we can find that about 1/3 of the 27 events seem to be close to the direction of Centaurus cluster. On the other hand, we cannot see obvious correlation with galaxies by eye in the AGASA data. In the results of both observatories, no UHE events have been detected at the highest energies in the direction of Virgo cluster, whose coordinate is at  $\sim (12\text{h}30\text{m}, +10^\circ)$ , as pointed out by Refs. [26, 27]. In the right figure, it is difficult to find galaxy clusters obviously because of the large number of galaxies projected to 2 dimensional space and the small number density of the IRAS galaxies at distant Universe due to the selection effect. Instead, the IRAS mask can be clearly seen. Several events of the PAO and AGASA are in the mask, but nevertheless we use all the events for analysis.

Fig.3 shows cross-correlation functions between the PAO events and the IRAS galaxies within (*upper panel*) and outside (*lower panel*)  $z = 0.018$ . For comparison, we also show cross-correlation functions calculated from randomly distributed cosmic rays with the same number of events, taking the anisotropic exposure of the PAO into account. The random event generations are performed 100 times, and we plot the mean values by dots and standard deviations by error bars. In each angular bin, the value of  $w_{\text{eg}}(\theta)$  for random events in each realization approximately follows the Gaussian distribution. Thus, the standard deviations can be regarded as  $1 \sigma$  statistical errors. We can check that the effects of the non-uniform exposures of the PAO and the IRAS mask are neatly corrected from the fact that all averaged values of  $w_{\text{eg}}(\theta)$  calculated from randomly distributed mock events are consistent with zero.

In the case of  $z \leq 0.018$ , the cross-correlation function of the PAO data is well beyond the error bars of random event distribution within  $15^\circ$ . Thus, we can find that the PAO data has significantly positive correlation with local galaxy distribution within  $z = 0.018$  at the angular scale of  $\leq 15^\circ$ . This means that UHECR deflection angles

with respect to the line of sight to the sources,  $\theta_{\text{obs}}$ , are less than  $15^\circ$ . On the other hand, in the lower panel, the PAO data is consistent with random distribution. Since the auto-correlation of the outside galaxies has a sharp peak at a small angular scale as explained afterward in this section, the consistency shows that there is no correlation between the PAO data and the outside galaxy distribution. These facts represent that a significant fraction of the 27 PAO events are injected from astrophysical sources within  $z = 0.018$ .

Fig.4 is the same figure as Fig.3, but for the AGASA data. The left panel shows the cross-correlation functions calculated from all published data of the AGASA ( $E > 40$  EeV, 57 events) and the right panel is those calculated using the AGASA data only above 57 EeV in the energy scale of the AGASA (23 events). In both panel, we cannot find the obvious signals of positive correlation like Fig.3.

We also consider the auto-correlation of galaxies and compare the angular scale of the cross-correlation to that of the auto-correlation. Fig. 5 shows the auto-correlation functions of galaxies within (*left*) and beyond (*right*)  $z = 0.018$  in the northern sky (*green*), southern sky (*blue*), and all sky (*red*). The error bars are estimated by 100 realizations of the isotropic distribution of galaxies with the same numbers. Both panels show the enhancement of the auto-correlations at small angular scales. Since the projection of galaxies  $z > 0.018$  is not isotropic, the cross-correlation test with galaxies beyond  $z = 0.018$  is justified.

The left panel shows that the angular scale of auto-correlations of the nearby galaxies is  $\sim 10^\circ$ . This scale is comparable with the angular scale of the cross-correlation in the southern sky. This fact shows that UHECR sources in the southern hemisphere are compatible with being distributed with the distribution of galaxies. However, we should notice that we cannot distinguish following two possibilities: UHECR sources themselves are distributed over the galaxy distribution, or the IGMF in the surrounding of UHECR sources deflects the trajectories of UHECRs and diffuse their arrival directions by the angular scale. In any case, we can conclude that the deflection angles of UHECRs are less than  $\sim 10^\circ$ .

In the northern sky, cross-correlation between UHECRs and nearby galaxies was not found as seen in Fig.4 while galaxies cluster at the small angular scale. We could suggest 2 possibilities for the lack of positive correlation. One is due to the energy-scale of the AGASA. The number of events with energies above 57 EeV (23 events) is comparable with that of the PAO (27 events) while the exposure of the AGASA is 7 times smaller than that of the PAO. This might be due to the difference of the energy-scale between the observations. If we require that the AGASA and PAO should observe the same UHECR spectrum, the energy-scale of the AGASA is expected to be shifted to lower energies and vice versa for the PAO. Thus, the 23 events include events with energies below 57 EeV. Since UHECRs with lower energies can arrive at the Earth from more distant sources, cross-correlation with nearby galaxies is weakened. Although galaxies outside  $z = 0.018$  cluster at a small angular scale, the signal is smaller than in the case of  $z \leq 0.018$  and thus the obvious signals of cross-correlation are not

found for  $z > 0.018$ . The deflections by the IGMF, which is neglected in this section, are also expected to affect the lack of cross-correlation for  $z > 0.018$  because of the relatively long propagation lengths of UHECRs. However, it is difficult to check this possibility because the difference of the energy-scale originates from not statistical errors but systematic errors.

The other is the lack of UHECR sources in nearby Universe in the northern sky, that is due to the difference between the northern and southern UHE Universe. However, it may be unlikely that there is the lack of UHECR sources despite the enhancement of the auto-correlation of nearby galaxies at a small angular scale if UHECR sources are astrophysical objects. This possibility can be discussed with a numerical simulation. In the next section, we discuss the reproducibility of the cross-correlation, especially for the AGASA, if UHECR sources are distributed to being comparable with the local galaxy distribution.

#### 4. Model Prediction

If UHECR sources are astrophysical objects, the arrival distribution of UHECRs is expected to be related to the local distribution of the sources [17, 18] or generally to galaxies in local universe [16, 19]. In this section, we test the reproducibility of cross-correlation function calculated from the observed data by simulating the arrival distribution of UHECRs based on a simple source model related to the galaxy distribution. The simulation takes the propagation of UHECRs in uniformly magnetized intergalactic space into account. The composition of UHECRs is assumed to be purely protons according to an implication based on the small deflections of UHECRs in the Galactic magnetic field (GMF) by the PAO [23]. Note that there are also claims that the composition of the highest energy cosmic rays includes a significant fraction of heavier components though there is uncertainty on hadronic interaction models in extensive air shower [36, 37, 38].

The mock UHECR source distribution is constructed by a method used in Ref.[55] based on the IRAS PSCz catalog of galaxies. This method allows us to construct source distribution related to the galaxy distribution. In the IRAS catalog, the distances of some nearby galaxies estimated by Ref.[39] are given. The distances of the other galaxies are determined from their recession velocities listed in the IRAS catalog, assuming the  $\Lambda$ CDM cosmology with  $H_0 = 71 \text{ km s}^{-1} \text{ Mpc}^{-1}$ ,  $\Omega_m = 0.3$ , and  $\Omega_\Lambda = 0.7$ , which are the Hubble constant at present, matter density and cosmological constant normalized by the critical density, respectively. The structured source distribution is adopted within 200 Mpc because such sources can contribute to about 90% of UHECR flux above  $6 \times 10^{19}$  eV. For the outside of 200 Mpc, source distribution is assumed to be isotropic. We adopt  $10^{-4} \text{ Mpc}^{-3}$  as the number density of UHECR sources, which can well reproduce the small-scale anisotropy observed by the PAO [40, 41]. The UHECR ejection power is assumed to be identical over all sources. We consider 100 mock source distributions with the same source number density changing the random seed. Each source is selected

with the same weight, not dependent on any property of galaxies like luminosity.

Methods for calculating the propagation of UHE protons and their arrival distribution follow those of Ref.[42]. UHE protons lose their energies by interactions with the CMB [43, 44] and their trajectories are deflected by the IGMF during their propagation. The IGMF is assumed to be a turbulent field with the Kolmogorov spectrum. The coherent length,  $l_c$ , is also assumed to be 1 Mpc, which is much larger than values indicated by Ref. [53] and used in Ref. [19]. The strength of the IGMF,  $B$ , is a free parameter since it is poorly known. The propagating protons interact with the CMB and lose their energies through photopion production and Bethe-Heitler pair creation. For pair creation, we adopt an analytical fitting function given by Ref. [45] to calculate the energy-loss rate in isotropic photons. Photopion production is treated as a stochastic process, and the interaction length calculated by an event generator SOPHIA [46] is adopted. The propagating protons also lose their energies through adiabatic energy-loss due to the cosmic expansion, but it is neglected in this study because this is not important for protons with energies above  $10^{19}$  eV. We consider UHE protons with  $10^{19}$ - $10^{22}$  eV. 5,000 protons are injected in each of 30 energy bins, that is 10 bins per decade of energy, from a source, and their trajectories and energies are calculated. The energies and deflection angles of protons are recorded at every 1 Mpc for  $d \leq 100$  Mpc while at every 10 Mpc for  $d > 100$  Mpc where  $d$  is the distance from the source, and their frequency distributions are constructed. The frequency distributions at a certain distance can be regarded as those of arriving protons from a source with that distance. Based on these frequency distributions, a given source distribution, and a given injection spectrum, the arrival distribution of mock UHE protons can be simulated. A power-law spectrum for UHECR injection,  $E^{-\alpha}$ , is assumed. We set  $\alpha = 2.6$  which is well reproduce the observed UHECR spectra above  $10^{19}$  eV. Note that all results are almost independent of the detailed value of  $\alpha$ , as long as  $\alpha$  is around 2-3, because a spectral shape at the highest energy level is dominantly determined by the GZK mechanism. We also consider the errors in arrival direction of the UHECR experiments. The angular distribution of the error is assumed to be a 2 dimensional Gaussian distribution with zero mean and the standard deviation equal to the detector resolution, which is  $1.0^\circ$  for the PAO and  $1.8^\circ$  for the AGASA.

Fig. 6 shows the cross-correlation functions of the IRAS galaxies with  $z \leq 0.018$  and UHE protons simulated for  $B = 0.1$  (*red*),  $1.0$  (*green*), and  $10.0$  nG (*blue*). The error bars represent standard deviations which are estimated from event realizations. The event realization is performed 1 time for every source distribution. Thus, the error bars include the error due to not only the finite number of events but also the sampling of galaxies in the different realizations. The apertures of the PAO (*upper panel*) and the AGASA (*lower panel*) are taken into account. The number of events is set to the same as the observed data, shown in the figure. The histograms and the black error bars are the same as in the upper panels of Figs.3 and 4.

For the PAO, the mock data for the 3 different IGMF strengths reproduce cross-correlation consistent with the observed data within the standard deviations. Thus, the

distribution of UHECR sources is evenly compatible with the local galaxy distribution in the southern hemisphere.

In principle, the cross-correlation of the observed data allows constraining the strength of IGMF because stronger IGMF deflects more the trajectories of protons and loses cross-correlation at a small angular scale. As we expect, the averages of the cross-correlation functions for  $B = 10.0$  nG are smaller than those for  $B = 1.0$  nG at a small angular scale in this figure. However, unfortunately, the difference between the averages in the 2 models is much smaller than the error bars. Thus, the discussion on the difference is only qualitative due to large error bars and we cannot distinguish the IGMF strength with sufficient significance.

It has a reason that the prediction for  $B = 0.1$ nG is almost the same as that for  $B = 1.0$ nG though the difference between the two is within the error bars. The reason is the finite resolution of cosmic ray arrival directions by UHECR observatories, typically  $\sim 1^\circ$ . Typical deflection angle of UHE proton is represented as

$$\theta_{\text{cr}}(E, d) \simeq 0.4^\circ Z \left( \frac{E}{60 \text{ EeV}} \right)^{-1} \left( \frac{d}{100 \text{ Mpc}} \right)^{1/2} \left( \frac{l_c}{1 \text{ Mpc}} \right)^{1/2} \left( \frac{B}{0.1 \text{ nG}} \right), \quad (6)$$

where  $d$  is the distance of a UHECR source. Note that the formula shows a typical angle between initial and final velocity of a propagating proton,  $\theta_{\text{cr}}(E, d)$ . Typically,  $\theta_{\text{obs}}$  is about a half of  $\theta_{\text{cr}}(E, d)$ .  $\theta_{\text{obs}}$  for  $B = 0.1$  nG is smaller than the angular resolution. Thus, the IGMF strength less than a few times 0.1 nG cannot be resolved by currently operating UHECR observatories. Note that it is possible that IGMF with the strength of  $\sim 1$  nG is not distinguishable if  $l_c$  smaller than 1 Mpc is realized in the Universe.

For the AGASA, the mock data almost reproduce the observational data within the standard deviations. The cross-correlation function of the AGASA can be reproduced by UHECR sources distributed with being comparable to galaxy distribution, especially within the angular scale of  $\sim 10^\circ$ . Thus, the lack of cross-correlation at a small angular scale in the AGASA data is still within errors. This means that the lack of UHECR sources in nearby northern sky is not always needed at present. When we watch cross-correlation functions at a larger angular scale, we find that the mock data predict slightly more positive signals than the observational data. A cause of this small discrepancy might be a simplicity of our source model. In our source model, the number density of UHECR sources is assumed to be constant in the whole Universe. If the number density of UHECR sources at a distant universe is relatively larger than at the local universe, cross-correlation between the distribution of local galaxies and the arrival directions of UHECRs is expected to become smaller, and may be fitted to that calculated from the observed data better. Although we would like to construct an improved source model in which a radial profile of the source number density is taken into account, we have little knowledge of UHECR sources. Thus, it will be studied when the number of detected events increases in the northern hemisphere and more information on UHECR sources can be obtained. The energy-scale might be a cause too because cosmic rays with lower energies can reach the earth from more distant sources. This gives a sense that correlation with nearby galaxies is weaken.

We also investigate cross-correlation between all-sky arrival distribution of both the PAO and AGASA data, and the IRAS galaxies with  $z \leq 0.018$ . For the combination of the two experimental data, the difference of energy-scale must be corrected. The energy spectra reconstructed by several experiments are different at the highest energy range (see Fig.5 in Ref. [47]) since UHECR experiments has a systematic error of  $\sim 30\%$  on energy determination. Following Ref.[49], a dip-calibration method, we shift UHECR energies of the AGASA data by 10% to lower energies. The dip-calibration method requires the injection spectrum of protons with  $\alpha = 2.6$ , which is used throughout this section. On the other hand, the energy spectrum of the PAO is not consistent with the calibrated spectra of the other experiments even if the energies are shifted maximally within systematic energy errors ( 22% [50]) [47]. Thus, we shift the PAO data by 50% to higher energies to be consistent with the shifted flux of the other experiments [47]. Then, we adopt  $8.55 \times 10^{19}$  eV as an energy threshold of events used, which corresponds to  $5.7 \times 10^{19}$  eV in the original energy-scale of the original PAO. As a result, we use all of the 27 PAO data and 9 events of the AGASA events whose original energies are above  $9.5 \times 10^{19}$  eV. The 9 events are shown in red in Fig. 2. Note that in a recent paper by the PAO their energy scale is slightly corrected to higher energies slightly [51], but the event data with the energies have not been published yet. Thus, we do not use the new energy scale.

Fig.7 represents cross-correlation functions calculated from the combined data (*histogram*), randomly distributed events (*black*), and mock UHE protons (*colors*). Comparing the histogram and black data (the same discussion in Figs.3 and 4), we find a significant positive correlation signal within  $8^\circ$ . This angular scale is comparable with the angular scale of the auto-correlation of nearby galaxies in all sky, and thus the all-sky data also indicates that the distribution of UHECR sources is related to the distribution of local galaxies. The 3 IGMF model predictions are consistent with the observed data within the standard deviations. Although UHECRs in the northern hemisphere are still controversial, this all-sky analysis indicates that the observed highest energy cosmic rays are consistent with a scenario in which their source distribution is associated with nearby galaxy distribution.

Finally, we comment on a possibility that the large error bars are reduced and we can constrain the IGMF strength by future observations. The error bars originate from both the finite number of observed events and the sampling of galaxies. The former error can decrease by increasing the number of events, while the latter error does not decrease. We checked the possibility by simulating 200 mock protons above  $\sim 60$  EeV. As a result,  $B = 10.0$  nG and  $B = 1.0$  nG are not distinguishable because of the latter error is left.

## 5. Discussion & Conclusion

In this paper, we have investigated spatial correlation between the arrival directions of the highest energy cosmic rays observed by the PAO and AGASA, and the IRAS

galaxies as a representative of the local structure of the universe. For statistical analysis, we adopted a cross-correlation function which can find the angular scale of the spatial correlation. This statistic need not to be set an artificial angular scale on correlation studies. We confirmed that the arrival directions of UHECRs above  $5.7 \times 10^{19}$  eV detected by the PAO are inconsistent with isotropic distribution and found that these have significant correlation with the galaxy distribution in the local universe inside  $z = 0.018$  within the angular scale of  $\sim 15^\circ$ . On the other hand, the AGASA data did not have obvious correlation with the IRAS galaxies. We also performed the same cross-correlation analysis on the whole sky using the combined data set of both the PAO and AGASA, and found the evidence of positive correlation within the angular scale of  $\sim 8^\circ$ . These results could be well reproduced by a source model that UHECR sources are distributed related to galaxies and the source number density is  $\sim 10^{-4}$  Mpc $^{-3}$ , taking propagation process in magnetized intergalactic space into account. These indicate that the distribution of UHECR sources are related to that of galaxies.

An important point of the results in this study is the angular scale in which the correlation is positive. We showed that the combined data has positive correlation compared to random event distributions within  $\sim 8^\circ$  in Section 4. This scale is comparable with the angular scale of the auto-correlation of galaxies within  $z = 0.018$ . Thus, we cannot distinguish the origin of the cross-correlation scale; the deflection angles of UHECRs in the IGMF or the spread of UHECR source distribution, but the result provides us with an upper limit of  $\theta_{\text{obs}}$ . It enables us to constrain several structured IGMF models. Several simulations of the LSS formation with magnetic field have been performed and have applied to the studies of UHECR propagation in the local universe [52, 53, 54], but the resultant magnetic structures are different except the centers of clusters. Among the three simulation results, 70% of protons reach the Earth with  $\theta_{\text{obs}} \geq 15^\circ$  even for the energies above  $10^{20}$  eV in an IGMF model of Ref. [52], in which only sources are strongly magnetized. Such large deflection angles are inconsistent with the angular scale of the spatial correlation estimated in this study. Thus, the magnetic structure in local Universe proposed by Ref. [52] is not consistent with the PAO data. Note that the authors of Ref. [52] pointed out the uncertainty of observer positions in their simulated universe (in other words, the magnetic structure of local Universe). The angular scale gives information on a magnetic field in local Universe

The angular scale of positive correlation against random event distribution also have information on the composition of UHECRs at the Earth, though interpretation depends on the results of the LSS formation simulations. Since UHECR sources are expected to be associated with dense structures, like clusters of galaxies and filamentary structures, propagating UHECRs are affected by magnetic fields in these structures. A LSS simulation by Ref. [54] showed that the filamentary structure has relatively strong magnetic field up to 10 nG. A simple but structured IGMF model developed in Ref. [55] also reproduce such structures. Propagating protons above  $6 \times 10^{19}$  eV in the magnetic structure by Ref. [54] is deflected by less than  $\sim 10^\circ$ , which is comparable with the angular correlation scale. When we assume heavy composition of UHECRs, like irons,

the deflection angles of UHECRs are a few tens times larger than protons. This conflicts with our estimated angular correlation scale. Thus, protons or light nuclei are favored as the composition of the highest energy cosmic rays if the IGMF models proposed by Refs. [54, 55] are real. On the other hand, a simulation by Ref. [53] predicted the filamentary structure with the IGMF strength of 0.1-1 nG and the volume fraction with the strength of magnetic field larger than 1nG is much smaller than the other 2 simulations. Thus, heavy nuclei-dominated composition is allowed if the IGMF model of Ref. [53] is real.

Another approach to estimate the strength of intervening magnetic field is the measurement of the separation angle between real UHECR sources and the arrival directions of UHECRs from them. The authors of Ref. [56] estimated the IGMF strength by using the correlation scale proposed by PAO ( $\sim 3.1^\circ$ ) as sub-nG assuming the PAO-correlated AGNs are real UHECR sources, though the assumption itself is controversial at present. When several sources are identified in the future, more detailed approaches to the magnetic field can be performed like Ref. [56].

In fact, it has shown that the GMF significantly contributes to the deflection angles of UHECRs [55, 57, 58, 59, 60, 61, 62]. Ref. [62] showed that the trajectories of UHE protons with  $\sim 6 \times 10^{19}$  eV are deflected by  $\sim 4^\circ$  on average in BS models except for protons arriving from the direction of the Galactic center. The deflection pattern is complicated and dependent on the arrival directions of protons. Also, GMF could affect the arrival directions of protons not only arriving near the Galactic plane but also arriving far from the Galactic plane [62]. In this situation, we completely neglected GMF and adopted all data without removing events with arrival directions near the Galactic plane as a first step in this study. The statistical analysis taking GMF into account is a next target of our study.

Finally, we comment on the calibration of the energy-scale. When we discussed the cross-correlation using the combined data, the energies of the AGASA data were shifted by 10% to lower energies and those of the PAO data were shifted by 50% to higher energies on the assumption of the dip-calibration, a physically motivated calibration method [47, 48]. However, the energy-shift of the PAO data is larger than its systematic uncertainty of 22% [23, 50] while the shift of the AGASA is within its systematic uncertainty [31, 63]. If the spectral dip at around  $10^{19}$ eV is generated by pair-creation interaction with the CMB, either/both experiments possibly underestimate the uncertainty on the energy determination. On the other hand, if we assume that the energy-scale of the HiRes is correct, the energy spectra of all UHECR observatories can be consistent by shifting the energies of each experimental data within each systematic uncertainty [64]. In this standpoint, we can interpret the spectral ankle not as the pair-creation dip but as the transition point from Galactic to extragalactic cosmic rays. The precise determination of the position of the dip enables us to distinguish the two interpretations on the ankle. When the correlation with extragalactic objects is investigated with combined data sets of observations of both the northern and southern hemispheres, as we have done, the calibration of the energy-scale is important because the GZK radius of protons in energy range from  $6 \times 10^{19}$  to  $10^{20}$  eV is sensitive to their

energy. Precise energy determination is required in order to develop charged particle astronomy. A consensus between the energy-scales of the experiments is required.

Now the PAO and Telescope Array [65] are operating and Extreme Universe Space Observatory (JEM-EUSO) [66] and the northern site of the PAO [67] are proposed. These experiments will not only accumulate much more statistics of UHECR events, but also determine the energy-scale precisely by more understanding physics in extensive air shower. We will be able to discuss UHECR sources more precisely in the near future.

### **Acknowledgments**

We are grateful to Susumu Inoue and Tokonatsu Yamamoto for useful discussions. The works of H.T., T.N, and K.Y. are supported by Grants-in-Aid from JSPS Fellows. The work of K.S. is supported by Grants-in-Aid for Scientific Research provided by the Ministry of Education, Culture, Sports, Science and Technology (MEXT) of Japan through Research Grants S19104006. This work was also supported by World Premier International Research Center Initiative (WPI Initiative), MEXT, Japan.

- [1] Takeda M *et al* 1999 *Astrophys. J.* **522** 225
- [2] Tinyakov P G Tkachev I I 2001 *JETP Lett.* **74** 445
- [3] Tinyakov P G Tkachev I I 2002 *Astropart. Phys.* **18** 165
- [4] Gorbunov D S *et al* 2002 *Astrophys. J.* **577** L93
- [5] Smialkowski A Giller M Michalak W 2002 *J. Phys. G: Nucl. Part. Phys.* **28** 1359
- [6] Singh S Ma C Arons J 2004 *Phys. Rev. D* **69** 063003
- [7] Saunders W *et al* 2000 *Mon. Not. Roy. Astron. Soc.* **317** 55
- [8] Hague J D *et al* 2007 *Astropart. Phys.* **27** 134
- [9] Gorbunov D S Troitsky S V 2005 *Astropart. Phys.* **23** 175
- [10] Stanev T *et al* 1995 *Phys. Rev. Lett.* **75** 3056
- [11] Uchihori Y *et al* 2000 *Astropart. Phys.* **13** 151
- [12] Stanev T 2008 *preprint* arXiv:0805.1746
- [13] Abbasi R U *et al* 2005 *Astrophys. J.* **623** 164
- [14] Abbasi R U *et al* 2007 *Astropart. Phys.* **27** 512
- [15] Abbasi R U *et al* 2006 *Astrophys. J.* **636** 680
- [16] Waxman E Fisher K B Piran T 1997 *Astrophys. J.* **483** 1
- [17] Yoshiguchi H Nagataki S Sato K 2003 *Astrophys. J.* **592** 311
- [18] Takami H Sato K 2008 *Astrophys. J.* **678** 606
- [19] Kashti T Waxman E 2008 *JCAP* **05** 006
- [20] Greisen K 1966 *Phys. Rev. Lett.* **16** 748
- [21] Zatsepin G T Kuz'min V A 1966 *JETP Lett.* **4** 78
- [22] Abraham J *et al* 2007 *Science* **318** 938
- [23] Abraham J *et al* 2008 *Astropart. Phys.* **29** 188
- [24] Veron-Cetty M P Veron P 2006 *Astron. & Astrophys.* **455** 773
- [25] Moskalenko I V *et al* 2009 *Astrophys. J.* **693** 1261
- [26] Gorbunov D S *et al* 2008 *JETP Lett.* **87** 461
- [27] Gorbunov D S *et al* 2008 *preprint* arXiv:0804.1088
- [28] Abbasi R U *et al* 2008 *Astropart. Phys.* **30** 175
- [29] George M R *et al* 2008 *Mon. Not. Roy. Astron. Soc. Lett.* 388 L59
- [30] Ghisellini G *et al* 2008 *MNRAS* **390** L88
- [31] Hayashida N *et al* 2000 *Astron. J.* **120** 2190
- [32] Sommers P 2001 *Astropart. Phys.* **14** 271
- [33] Peebles P J E 1980 *The Large-Scale Structure of the Universe* Princeton University Press
- [34] Landy S D Szalay A S 1993 *Astrophys. J.* **412** 64
- [35] Blake C *et al* 2006 *Mon. Not. Roy. Astron. Soc.* **368** 732
- [36] Unger M *et al* 2007 *preprint* arXiv:0706.1495
- [37] Engel R *et al* 2007 *preprint* arXiv:0706.1921
- [38] Glushkov A V *et al* 2008 *JETP Lett.* **87** 190
- [39] Rowan-Robinson M 1988 *Sp. Sci. Rev.* **48** 1
- [40] Takami H Sato K 2009 *Astropart. Phys.* **30** 306
- [41] Cuoco A *et al* 2008 *preprint* arXiv:0809.4003
- [42] Yoshiguchi H *et al* 2003 *Astrophys. J.* **586** 1211 (Erratum **601** (2004) 592)
- [43] Berezhinsky V Grigorieva S I 1988 *Astron. & Astrophys.* **199** 1
- [44] Yoshida S Teshima M 1993 *Prog. Theor. Phys.* **89** 833
- [45] Chodorowski M J Zdziarske A A Sikora M 1992 *Astrophys. J.* **400** 181
- [46] Mucke A *et al* 2000 *Comput. Phys. Commun.* **124** 290
- [47] Berezhinsky V 2007 *preprint* arXiv:0710.2750
- [48] Aloisio R *et al* 2007 *Astropart. Phys.* **27** 76
- [49] Berezhinsky V Gazizov A Z Grigorieva S I 2005 *Phys. Lett. B* **612** 147
- [50] Dawson B *et al* 2007 *preprint* arXiv:0706.1105
- [51] Abraham J *et al* 2008 *Phys. Rev. Lett.* **101** 061101

- [52] Sigl G Miniati F Ensslin T A 2004 *Phys. Rev. D* **70** 043007
- [53] Dolag K *et al* 2005 *JCAP* **01** 009
- [54] Das S *et al* 2008 *Astrophys. J.* **682** 29
- [55] Takami H Yoshiguchi H Sato K 2006 *Astrophys. J.* **639** 803 (Erratum **653** (2006) 1584)
- [56] De Angelis A Persic M Roncadelli M, 2008 *Mod. Phys. Lett. A* **23** 315
- [57] Stanev T 1997 *Astrophys. J.* **479** 290
- [58] Medina-Tanco G A *et al* 1998 *Astrophys. J.* **492** 200
- [59] Alvarez-Muniz J Engel R Stanev T, 2002 *Astrophys. J.* **572** 185
- [60] Kachelriess M Serpico P D Teshima M 2007 *Astropart. Phys.* **26** 378
- [61] Yoshiguchi H Nagataki S Sato K 2004 *Astrophys. J.* **607** 840
- [62] Takami H Sato K 2008 *Astrophys. J.* **681** 1279
- [63] Takeda M *et al* 2003 *Astropart. Phys.* **19** 447
- [64] V. Berezhinsky, *private communication*
- [65] Fukushima M *et al* 2007 *Proc. 30th Int. Cosmic Ray Conf. (Merida)* # 955
- [66] Ebisuzaki T *et al* 2007 *Proc. 30th Int. Cosmic Ray Conf. (Merida)* # 831
- [67] Nitz De *et al* 2007 *Proc. 30th Int. Cosmic Ray Conf. (Merida)* # 180

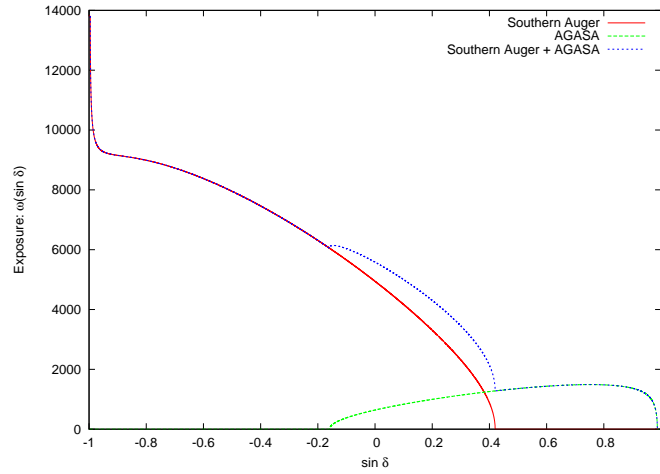


**Figure 1.** Declination ( $\delta$ ) dependence of the exposures of the PAO (*red*) and AGASA (*green*). The total exposures are  $9,000 \text{ km}^2\text{sr}$  for the PAO and  $1.3 \times 10^3 \text{ km}^2\text{sr}$  for the AGASA. The combined exposure is also shown (*blue*).

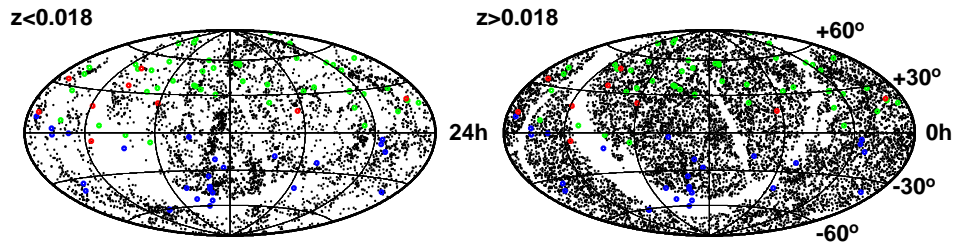


**Figure 2.** Distributions of the IRAS galaxies within (*left*) and outside (*right*) of  $z = 0.018$  with the arrival directions of the highest energy events detected by PAO (*blue points*) above  $5.7 \times 10^{19} \text{ eV}$  and AGASA (*green and red points*) above  $4.0 \times 10^{19} \text{ eV}$ . The red points represent the AGASA data above  $9.5 \times 10^{19} \text{ eV}$  in its energy-reconstruction scale and the green points are those below  $9.5 \times 10^{19} \text{ eV}$ .

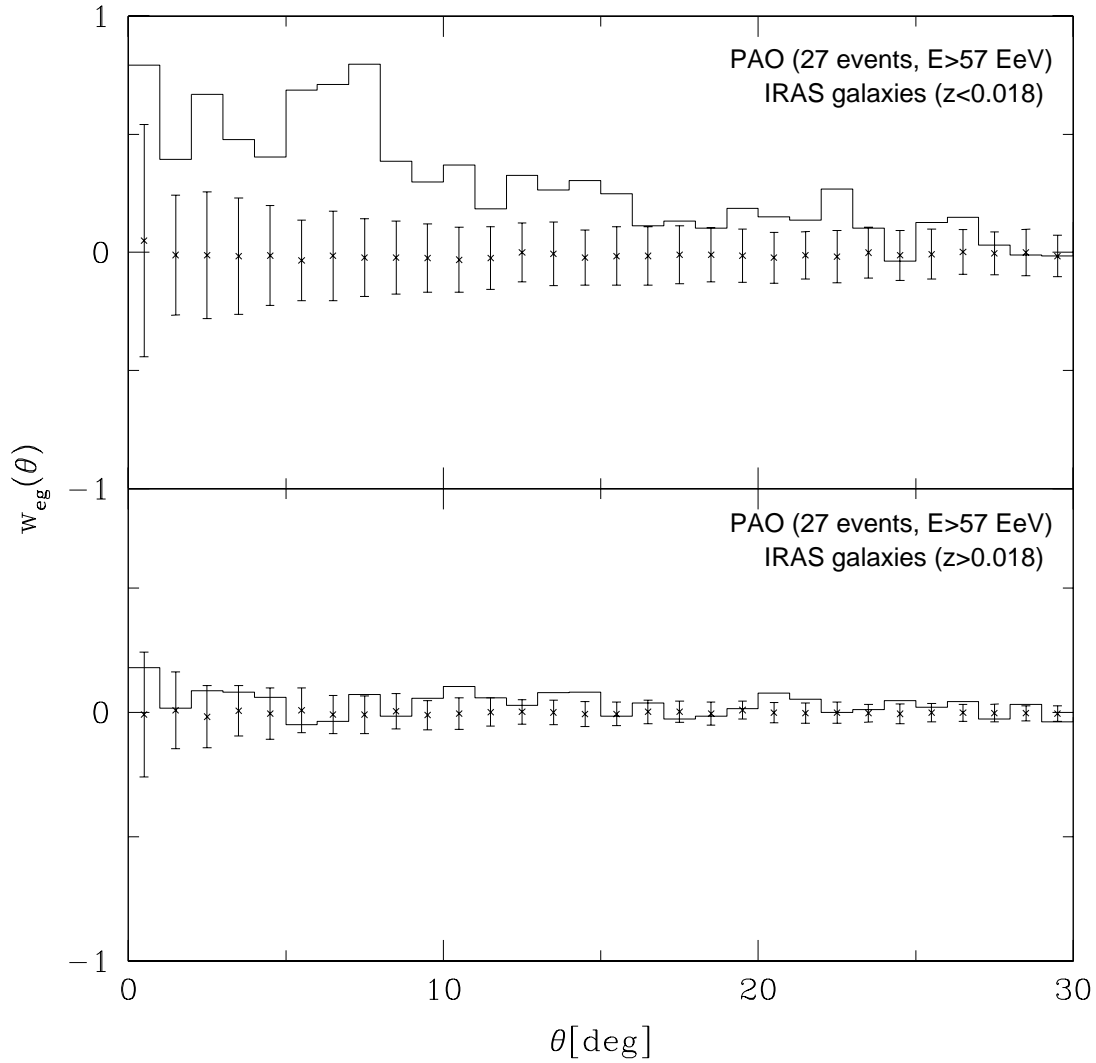


**Figure 3.** Cross-correlation functions,  $w_{\text{eg}}(\theta)$ , between the highest energy events detected by the PAO and the IRAS galaxies within (*upper panel*) and outside  $z = 0.018$  (*lower panel*). The histograms are  $w_{\text{eg}}(\theta)$  calculated from the observed data.  $w_{\text{eg}}(\theta)$  calculated from random distribution, taking the non-uniform exposure of the PAO into account, is also shown with the standard deviation due to the finite number of events.

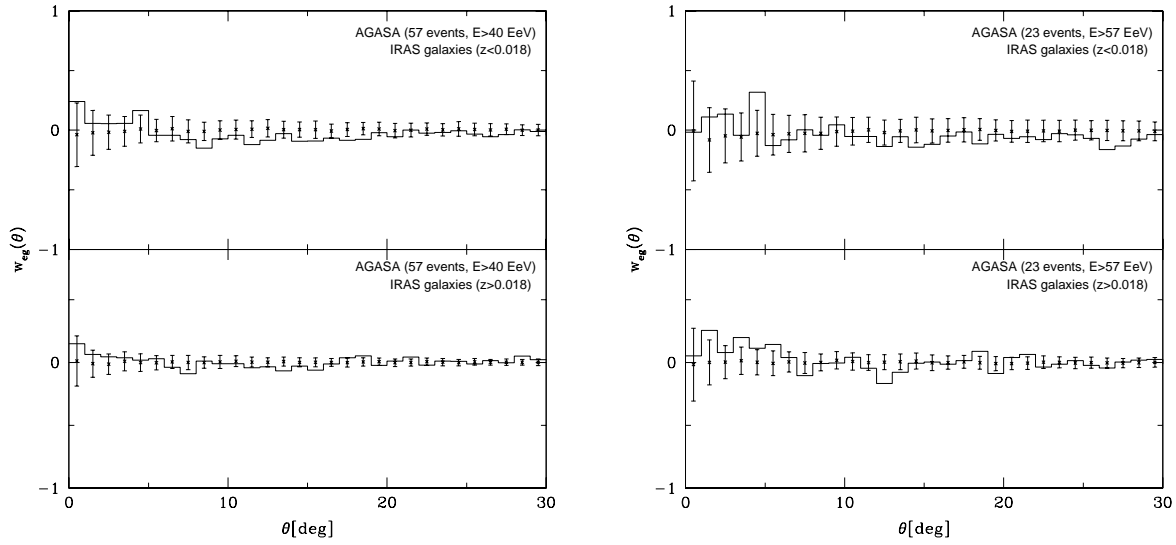


**Figure 4.** The same figures as Fig.3, but for the AGASA data. The threshold energies of events used are  $4.0 \times 10^{19}$  (left) and  $5.7 \times 10^{19}$  eV (right) respectively.

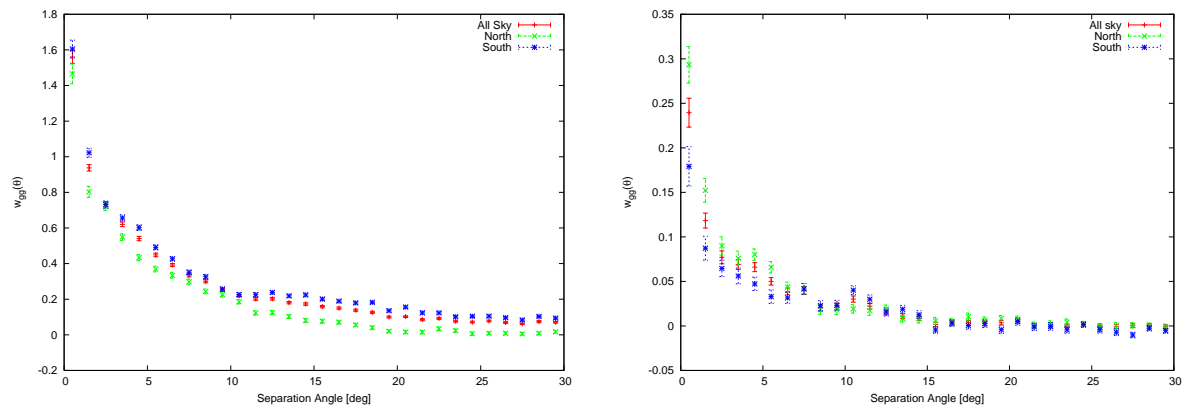


**Figure 5.** Auto-correlation functions of the IRAS galaxies within  $z = 0.018$  (left) and beyond  $z = 0.018$  (right) in the northern sky (green), the southern sky (blue), and all sky (red).

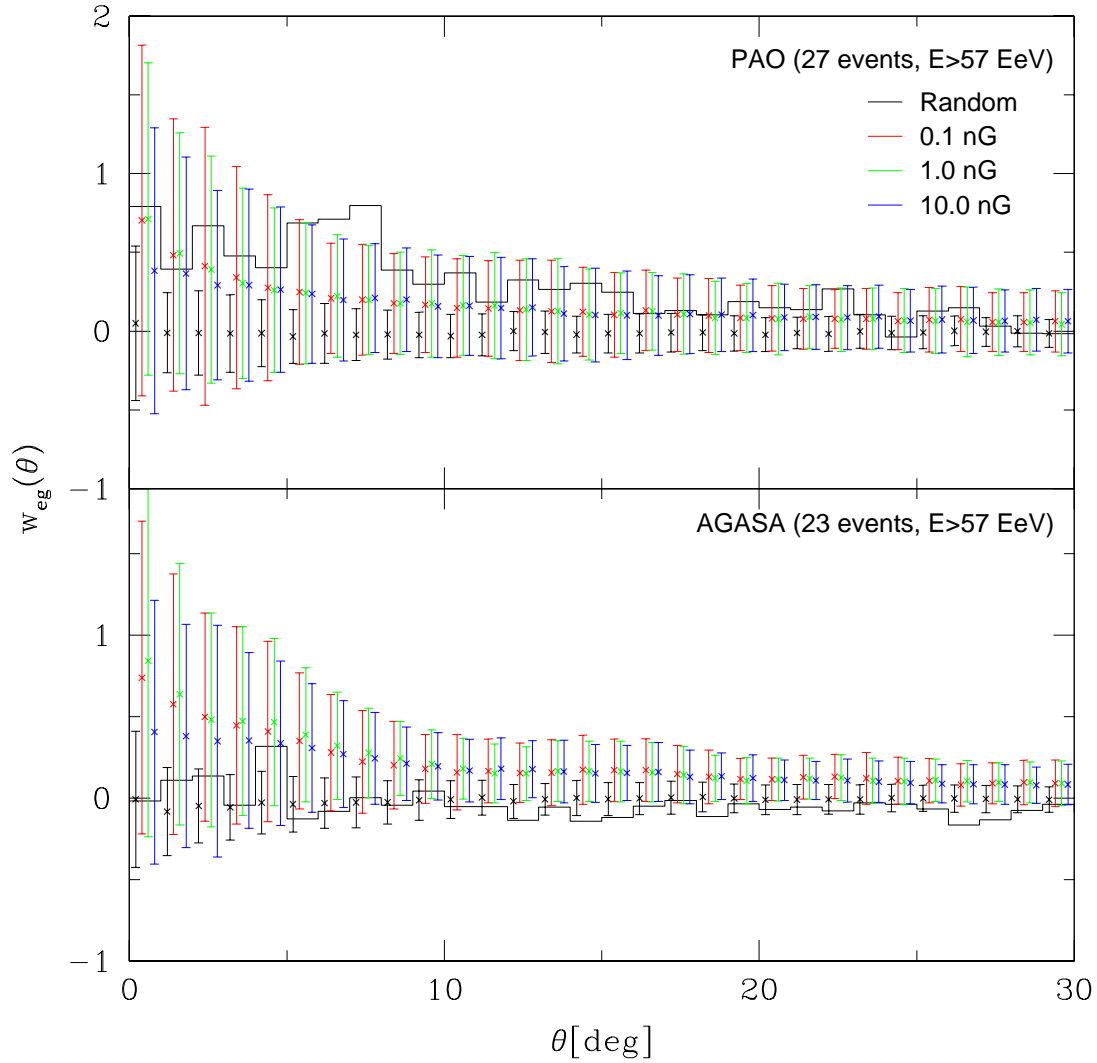


**Figure 6.** Cross-correlation functions predicted by our source model. The color points and error bars are in the case of  $B = 0.1$  (red), 1.0 (green), and 10.0 nG (blue) respectively. The histograms, and black points and error bars are the same as the upper panels of Fig.3 and Fig.4.

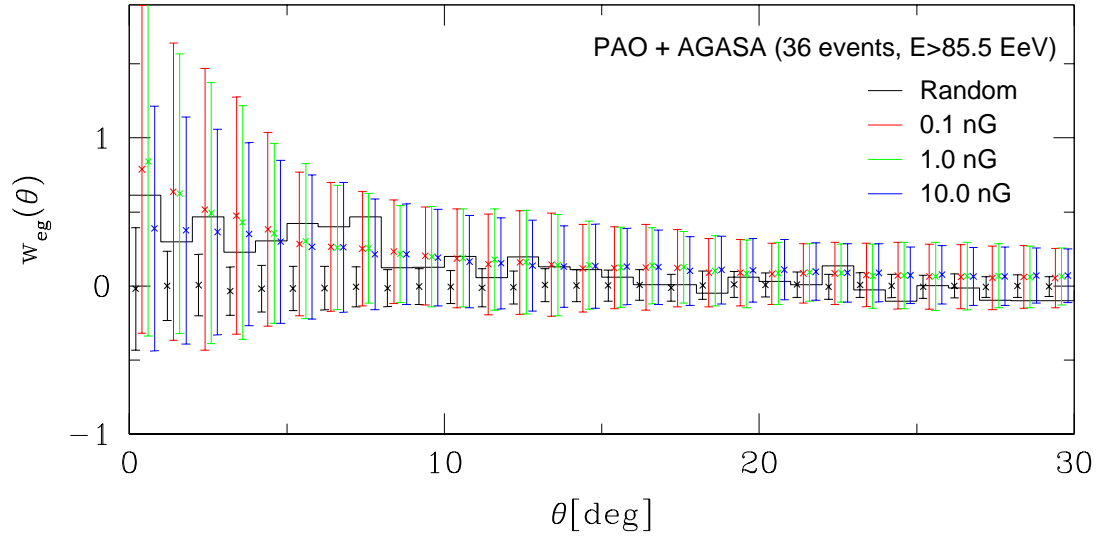


**Figure 7.** The same as Fig.6, but for the combined events.